Available online at www.sciencedirect.com
SCIENCE DIRECT®
Coordination Chemistry Reviews 249 (2005) 1766–1775
COORDINATION CHEMISTRY REVIEWS
www.elsevier.com/locate/ccr

Review

Recent advances in the shape control of inorganic nano-building blocks

Young-wook Jun [a], Jung-wook Seo [a], Sang Jun Oh [b], Jinwoo Cheon [a, *]

[a] *Department of Chemistry, Yonsei University, Schinchon-dong Seodaemun-gu, 120 749 Seoul, Republic of Korea*
[b] *Korea Basic Science Institute, 305333 Daejeon, Republic of Korea*

Received 1 October 2004; accepted 9 December 2004
Available online 5 February 2005

Contents

Abstract

Inorganic nanocrystals with certain geometries exhibit unique shape dependent phenomena and subsequent utilization of them as building blocks for the key components of nanodevices is of huge interest. Architecture of these nanocrystals can be simply classified by their dimensionalities: zero-dimensional (0D) quantum dots including spheres, cubes, and tetrahedrons, one-dimensional nanorods and wires, two-dimensional (2D) nanodiscs and plates, and other advanced shapes such as rod-based multipods and nanostars. Among them, one-dimensional (1D) structures are of current interest in materials chemistry not only because they exhibit novel optical properties arising from dimensional anisotropy, but also because they can be utilized as key materials in addressable two-terminal circuits for nanodevice applications. We describe here the current studies on a variety of one-dimensional semiconductor and metal oxide nano-building blocks obtained by liquid phase colloidal synthetic methods. Several mechanisms and critical parameters for nanocrystal shape guiding processes are carefully examined. Once we understand the guiding laws of nanocrystals growth, many new nano-building blocks will easily be tailored for the discovery of novel phenomena and also further exciting advancement of nanoscience and nanotechnology.

Keywords: Inorganic nanocrystals; Nano-building blocks; Shape control

1. Aspects of nanoscale building blocks

Nanocrystals that are usually regarded as "artificial atoms" are the basic units for nanoscale devices [1], and the design and operation of these devices will be easily accomplished by using nanocrystals with distinct sizes and shapes. By assembling and patterning nano-building blocks in a manner similar to assembling "Lego" blocks, the fabrication of future devices that are extremely fast, efficient, and small will be possible [2]. As with Lego blocks, various shapes and sizes of nano-building blocks will be required for the various components of the nanostructure.

* Corresponding author. Tel.: +82 2 212 35631; fax: +82 2 364 7050.
E-mail address: jcheon@yonsei.ac.kr (J. Cheon).

0010-8545/$ – see front matter © 2004 Elsevier B.V. All rights reserved.
doi:10.1016/j.ccr.2004.12.008

It has been found that size and shape of nanocrystals are key factors for the determination of their chemical and physical properties. Bulk materials have peculiar characters such as color, phase transition temperature, and band-gap. For example, gold has golden color and silver has metallic properties. In nanoscale regime, however, color of gold can be red, deep violet and blue [3] and silver can be an insulator depending on their sizes, shapes, or assemblies [2]. In other words, the size and shape of nanocrystals act as critical parameters for determining materials properties. If the precise control of size and shape of nanocrystals is possible, their chemical and physical properties can be manipulated as desired [4]. Then, these nanocrystals can be used as the building blocks for assembling and patterning future nanodevices. Therefore, the control of nano-building blocks is crucial for the success of future nanodevices.

Basic nano-building blocks can be classified by crystal symmetry and dimensionality. Spheres, icosahedrons, and cubes can be classified as zero-dimensional isotropic basic elements. These are of the most familiar shapes in the nanoworld. Semiconductor and metal nanospheres and C_{60} are in this group. Rods, cylinders with polygon shape, and wires are examples of one-dimensional anisotropic basic elements. These building blocks can be applicable for two-terminal circuit devices [5,6]. Carbon nanotubes are another good example of one-dimensional building blocks. Using cross-junctions of carbon nanotubes, nonvolatile random access memory devices are possible [7]. Discs, plates with polygon shape belong to two-dimensional anisotropic basic elements [3,8,9]. Examples of rather complex structured building blocks are star shaped and multi pod structures such as highly symmetric crosses [10].

There are several approaches to prepare nano-building blocks including gas phase syntheses and liquid phase syntheses. In the recent years, shape control of nano-building blocks through liquid phase synthesis has been extensively carried out, which includes metals, semiconductors, and ceramics.

In this review, we focus on the current achievements and perspectives in shape controlled synthesis of semiconductor and metal oxide nano-building blocks using liquid phase synthesis.

2. Current achievements and perspectives of nano-building blocks

At the early stage of researches on nano-building block synthesis, zero-dimensional shapes as regarded the most basic and symmetric shape including spheres and cubes have been extensively studied. In rather earlier period of research trends, nanocrystals were usually grown in a hydrolytic media in the presence of structured micelles [11]. Several semiconductor nanocrystals have been grown from aging processes of ionic precursors inside organic micelles. However, nanocrystals obtained by this method have relatively poor crystallinity or polydispersity in their size. As an alternative way to solve these problems, a thermal decomposition method of organometallic precursors under hot organic solution was adopted. At first, Brus and co-workers synthesized various II–VI semiconductor nanospheres with high colloidal stability with coordinating solvents (e.g., 4-ethylpyridine) [12], but size tunability and monodispersity of nanocrystals obtained were still poor. Bawendi and co-workers [13] successfully developed more advanced methodology to prepare various sized CdSe nanocrystals via the method of injecting a precursor solution containing dimethyl cadmium and trioctylphosphine selenide into a hot trioctylphosphine oxide (TOPO) solution. The size of nanocrystals varied from 1.2 to 12 nm with high monodispersity and crystallinity and the nanocrystals obtained were highly soluble in various organic solvents. Optical spectra clearly exhibit size dependent quantum confinement effects indicating high monodispersity and high crystallinity of nanocrystals.

The development of the precursor injection method into hot capping molecule solution also offers the opportunity to synthetically tune the crystal growth processes. By controlling growth variables such as temperature, the choice of capping molecules, precursor concentrations, crystalline phases of nuclei, and the choice of growth regime between kinetically controlled and thermodynamically controlled growth, various nano-building blocks with multi-dimensionalities have been yielded.

2.1. One-dimensional rods and wires

Recent studies on the shape control of nanocrystals have been highly focused on one-dimensional systems. Since one-dimensional rod growth is the fundamental step of anisotropic shape control, it may be possible to have further control of nano-building blocks with highly complex structures once we understand the shape guiding mechanisms of nanorods.

To generate one-dimensional nanocrystals, researchers have explored ‘one step in situ synthesis’ of 1D nanorods utilizing methods similar to those for the well-studied spherical nanocrystals. For example, the 1D colloidal rod based system of CdSe has been successfully demonstrated by Peng et al. [14] and Alivisatos and co-workers [15]. The use of binary capping molecules such as TOPO and hexylphosphonic acid (HPA) was effective for the generation of shape anisotropy in CdSe along with the nature of its intrinsic hexagonal structure. Recent studies on in situ anisotropic growth of the nanocrystals propose a growth process that is referred to as “oriented attachment”. Kotov and co-workers demonstrated the formation of CdTe nanowires via crystal dipole-induced self-assembly of CdTe nanospheres [16].

Another approach for liquid phase preparation of nanorods via a ‘two step seed mediated synthesis’. In the first step, spherical seed nanocrystals are synthesized and isolated. Precursors of desired 1D structure then chemically reduced in the presence of capping molecules where seed nanocrystals serve as nucleation points. Gold nanosphere direct growth of

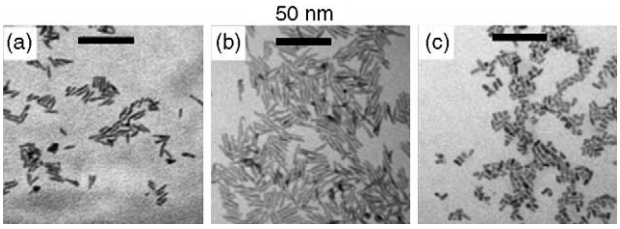

Fig. 1. CdSe nanorods grown using thermal decomposition of precursors in the presence of binary surfactants. (Reprinted in part with permission from ref. [14]. Copyright 2000 Nature.)

Si nanowires by seed catalytic growth in supercritical fluid was presented [17]. Although interface issues between the seed and growth materials have not been well resolved, this method has great potential for further advances of researches on 1D rod structured materials. The general applicability of this method to other materials needs to be further explored.

2.1.1. Groups II–VI semiconductors

Non-hydrolytic high temperature injection method can are heavily utilized for high quality nanorod synthesis. Peng et al. [14] and Alivisatos and co-workers [15] first reported CdSe nanorods via thermal decomposition of dimethylcadmium and trioctylphosphineselenide in a hot surfactant mixture of trioctylphosphine oxide and hexylphosphonic acid. In this synthesis, one-dimensional rod shaped structures result from preferential growth along the [0 0 1] direction of wurtzite CdSe that is promoted by a selective adhesion of HPA molecules on specific faces. With increasing HPA concentration, the nanocrystal shape evolves from spheres and short rods to long rods with high aspect ratios (Fig. 1).

On the other hand, Cheon and co-workers reported a simpler synthetic method using a single source precursor instead of dual sources. For example, zinc telluride nanorods were formed when a single source precursor, $Zn(TePh)_2$-TMEDA, decomposed in a hot amine surfactant mixture [18]. Anisotropic one-dimensional growth of metal sulfide nanocrystals including CdS, MnS, and PbS was also possible by thermal decomposition of stable single molecular precursors in a mono-surfactant system [10,19,20].

Hydrolytic synthesis of II–VI semiconductors also produces one-dimensional rod-shaped nanocrystals by shape transformations involving oriented attachment processes. Weller and co-workers have proposed an alignment and reorganization of zinc oxide nanocrystals via oriented attachment process [21] (Fig. 2(a)). In this synthesis, zinc acetate produces zinc oxide nanospheres through hydrolysis and aging processes. The nanospheres are then aligned and fused together in order to remove high-energy surfaces. Finally, reconstruction processes of the fused nanocrystal surfaces result in rod shaped nanocrystals with flat surfaces (Fig. 2(b)). Similar shape transformation processes were also observed in other II–VI semiconductor nanocrystals. Kotov and coworkers reported a shape transformation from sphere to rod by dipole-induced fusion of CdTe individual nanospheres

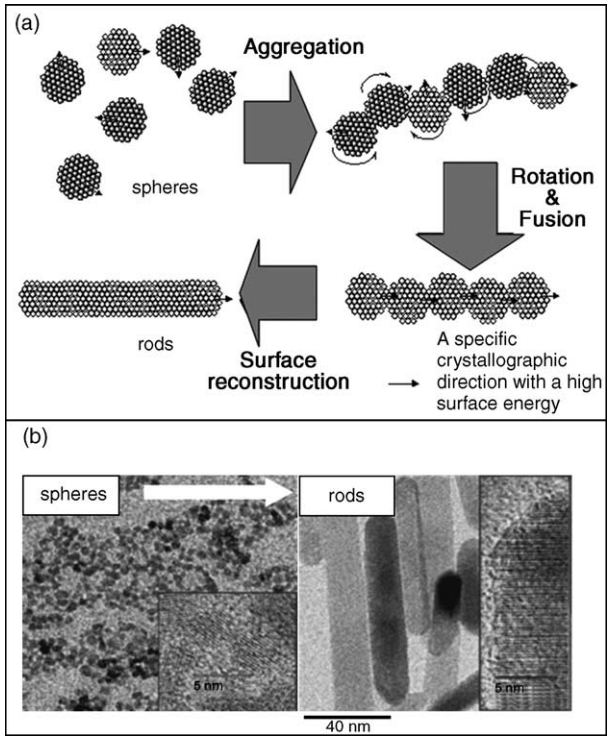

Fig. 2. (a) Schematic illustration of oriented attachment processes. (b) Shape transformation from ZnO nanosphere aggregates to nanorods. (Reprinted in part with permission from ref. [21]. Copyright 2002 Wiley–VCH.)

[16]. Zincblende CdTe spheres were first formed by reaction between Cd and Te precursors in aqueous solution. Then, CdTe spheres obtained were aligned through dipole interactions between nanocrystals. Finally, the nanospheres were fused together with a simultaneous crystal phase transition to wurtzite.

2.1.2. Groups III–V semiconductors

Unlike II–VI semiconductor systems that have been thoroughly studied, anisotropic shape control of III–V semiconductor nanocrystals has been very limited. This is most likely due to a greater degree of their covalent bonding nature and the absence of suitable precursors. Moreover, except for metal nitrides, III–V semiconductors favor isotropic zinc blende structures, and thus 0D nanocrystal growth is commonly preferred rather than rod growth [22]. Cheon and co-workers have shown that the crystalline phase of gallium phosphide nanocrystals can be chemically controlled by adopting suitable surfactants [23]. GaP semiconductors have two different crystalline phases that are in rotational isomerism, the zinc blende phase is a staggered conformation with [1 1 1] directions while the wurtzite phase is an eclipsed conformation with [0 0 1] directions (Fig. 3(a and b)) [22]. Zinc blende GaP is a thermodynamically stable phase that is sterically favored. Wurtzite GaP is a kinetically stable phase that is electronically favored due to the electrostatic interaction between geminal gallium and phosphine atoms when wurtzite GaP monomers approach on to the crystal surface. When sterically bulky ter-

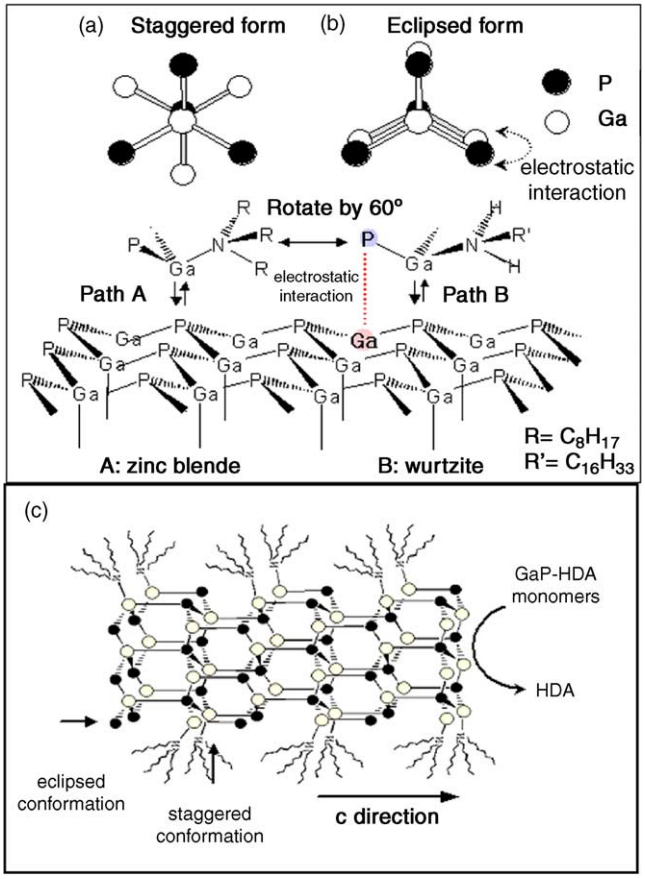

Fig. 3. Shape guiding processes of GaP nanocrystals. Steric and electronic effects on the crystalline phase (a and b) and the rod growth (c) of GaP nanocrystals. (Reprinted in part with permission from ref. [23]. Copyright 2002 American Chemical Society.)

tiary amines are used as capping molecules, the staggered conformation is highly favored due to the large steric hindrance between capping molecules and the crystal surface. Therefore, formation of zinc blende GaP nanospheres is favored (Fig. 3(a)). However, when sterically less hindered primary amines are present, steric energy difference between the eclipsed conformation and the staggered conformation is diminished. Steric effects on determining the binding geometry of incoming monomers are now small and electronic effects play a major role under a kinetically driven growth regime with a high monomer concentration. Therefore, formation of wurtzite GaP phase is facilitated (Fig. 3(b)). In short, the formation of a zinc blende structure is favored with highly steric ligands such as trioctylamine, while wurtzite is dominant under less bulky linear alkyl amines (e.g., hexadecylamine).

Once the crystalline phase is determined, subsequent kinetic growth yields different types of shapes, which is also affected by the stereochemistry of ligands. When wurtzite seeds are formed, sterically bulky TOA selectively binds to the other faces (e.g., {1 0 0} and {1 1 0} faces) with a staggered conformation rather than to the {0 0 2} faces and blocks growth on these faces. On the other hand, GaP–HDA complexes continuously supply monomers on the {0 0 1} faces with high surface energy, and therefore promote the growth in the *c*-direction of a rod structure (Fig. 3(c)).

III–V Semiconductor one-dimensional nanocrystals including InP, GaAs, and InAs can also be synthesized via solution–liquid–solid (SLS) processes [24] (Fig. 4). When semiconductor precursors decompose, precursor molecules generate monomers in solution. The monomers diffuse into liquid metal seeds and eventually precipitate and crystallize along a specific direction when the liquids seeds are super-saturated, inducing the formation of one-dimensional nanocrystals (Fig. 4(a)). Buhro and co-workers synthesized various III–V nanowires including GaAs, InP and InAs through the SLS processes (Fig. 4(b)), but the nanowires obtained have generally poor solubility and the control of nanowire length is very difficult. Banin and co-workers reported synthesis of soluble InAs nanorods and wires with controlled lengths and diameters through a modified procedure [25]. The injection of gold nanocrystal seeds together with precursors ($InCl_3$ and As(trimethylsilyl)$_3$) into hot capping molecule solution, trioctylphosphineoxide, yielded InAs nanorods with various lengths of nanorods (Fig. 4(c)). The nanorods obtained exhibits length-dependent quantum confinement effects in their optical spectra (Fig. 4(d)).

2.1.3. Group IV semiconductors

In the case of group IV semiconductor systems, it is extremely difficult to obtain nanorods by typical solution based precursor injection methods due to their highly covalent character. In contrast, under gas phase based syntheses such as chemical vapor deposition, one-dimensional silicon and germanium wires can be easily obtained on a substrate using vapor–liquid–solid (VLS) growth mechanisms [26]. In VLS growth mechanisms, monomers can form an alloy in equilibrium with their pure solid in a catalytic seed and one-dimensional group IV semiconductor nanowire is expelled from the seed as they reach supersaturation. Similar approach can be used for generating colloidal nanowires. Monomers in solution diffuse onto the catalytic seeds and form an alloy with them. As the dissolution of monomers into the seed increases, the supersaturated pure solid nanowire grows out of the catalytic seed. For example, in the supercritical hexane fluid environment, Ge nanowires have been obtained via gold catalysts by Hanrath and Korgel [27] (Fig. 5). Above 300 °C, Ge and Au can form an alloy in equilibrium with pure solid Ge. Monomers made by thermal degradation of Ge precursor dissolute into Au nanocrystals until reaching a Ge:Au alloy supersaturation and pure solid Ge is expelled from the Au seeds. Size-monodispersed Au nanocrystals are necessary to achieve nanowire growth. By changing the reaction pressure, it is possible to control the growth direction of nanowires.

Gerion et al. reported two-step synthesis of Ge nanorods through a high temperature precursor decomposition method under a high pressure (∼200 mTorr) [28]. Although the anisotropic growth mechanism of the germanium nanocrys-

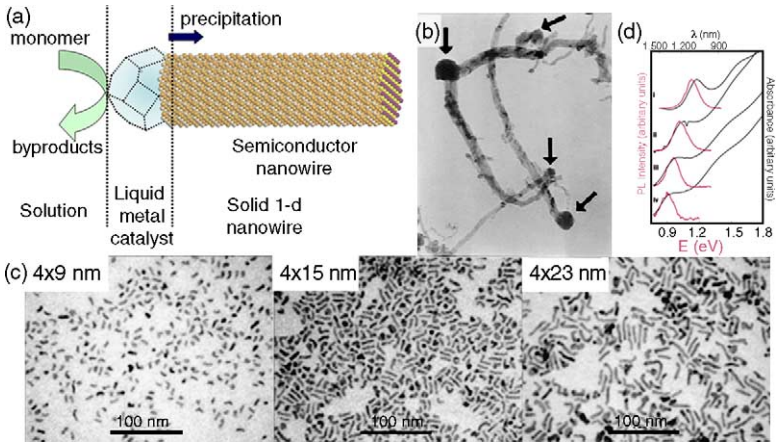

Fig. 4. (a) Schematic of solution–liquid–solid (SLS) growth process and (b) InP nanowires. (Reprinted in part with permission from ref. [24]. Copyright 1997 American Chemical Society.) (c) InAs nanorods (Reprinted in part with permission from ref. [25]. Copyright 2003 Nature.) (d) Length dependent optical properties of InAs nanorods: 4 nm nanospheres (i), 4 nm × 9 nm (ii), 4 nm × 15 nm (iii), and 4 nm × 21 nm nanorods. (Reprinted in part with permission from ref. [25]. Copyright 2003 Nature.)

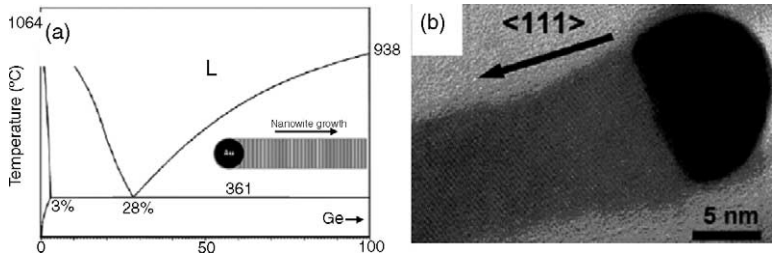

Fig. 5. SLS growth of Ge nanowires. (a) Phase diagram between germanium and gold and (b) a HRTEM image. (Reprinted in part with permission from ref. [27]. Copyright 2002 American Chemical Society.)

tals is unclear yet, this implies that synthesis of anisotropic Ge nanorods is possible without metal seeds.

2.1.4. Metal oxides

Transition metal oxides consist of an important group of materials used in white pigment, electronic ceramics, cosmetics, supports in catalysis, and as photocatalysts. Nanostructured titania are of particular interest with potential applications as solar cell materials. Chemseddine and Moritz demonstrated elongated TiO_2 nanocrystals synthesized by hydrolysis and polycondensation of titanium alkoxide [$Ti(OR)_4$] in the presence of tetramethyl ammonium hydroxide (Me_4NOH) as a stabilizer and reaction catalyst (Fig. 6) [29]. Organic cations stabilized the anatase polyanionic core and increased monomer flux induced one-dimensional growth of the titania nanocrystals.

Penn and Banfield also reported naturally aligned titania nanocrystals under hydrothermal conditions [30], by adapting an oriented attachment mechanism into the nanocrystal development (Fig. 7). Hydrothermal treatment of titanium alkoxide precursors produces diamond shaped anatase titania nanocrystals. The nanocrystals were truncated with three different kinds of faces: {0 0 1}, {1 2 1}, and {1 0 1} faces. Because the (0 0 1) face has the largest number of dangling bonds and the (1 0 1) face has the lowest number

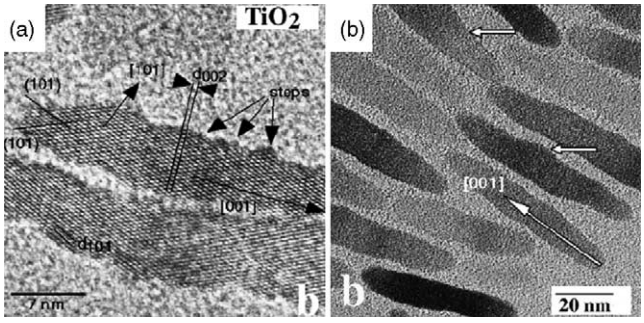

Fig. 6. One-dimensional titanium dioxide nanorods. (a) A large area TEM image and (b) a HRTEM image. (Reprinted in part with permission from ref. [29]. Copyright 1999 Wiley–VCH.)

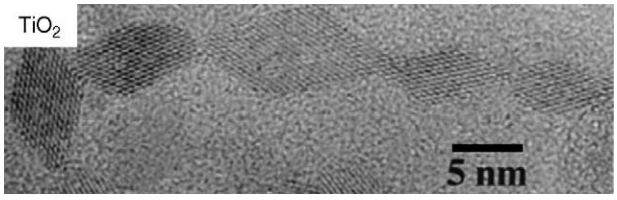

Fig. 7. Naturally aligned titanium dioxide nanocrystals. (Reprinted in part with permission from ref. [30]. Copyright 1999 Elsevier.)

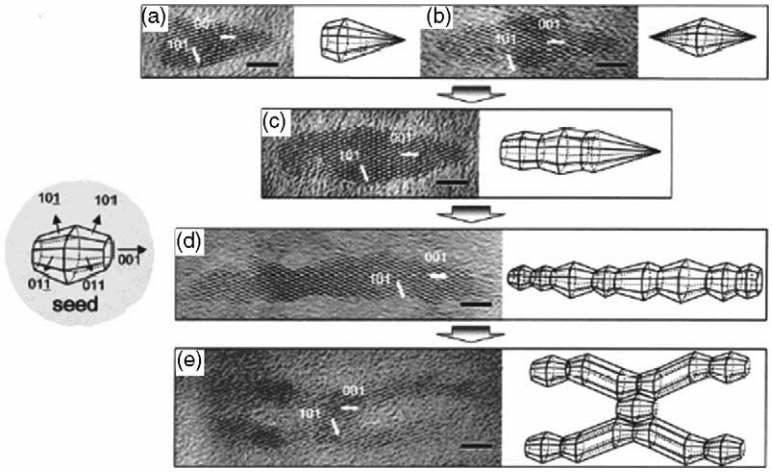

Fig. 8. High resolution TEM analyses and simulated three-dimensional (3D) shape of (a) a bullet, (b) a diamond, (c) a short rod, (d) a long rod, and (e) a branched rod. The long axes of the nanocrystals are parallel to the *c*-axis of the anatase structure, while the nanocrystals are faceted with {1 0 1} faces along the short axes. Hexagon shapes (the [0 1 0] projection of a truncated octagonal bipyramid) truncated with two {0 0 1} and four {1 0 1} faces are observed either at the one end or at the center of the nanocrystals. The branched shape is a result of the growth along [1 0 1] directions starting from the hexagon shape. Scale bar = 3 nm. (Reprinted in part with permission from ref. [31]. Copyright 2003 American Chemical Society.)

of dangling bonds, the surface energy of the (0 0 1) face is higher than that of the (1 0 1) face. When a sufficient thermal energy was supplied to the system, the removal of high-energy surfaces was thermodynamically favorable. Thus, fusion between diamond-shaped nanocrystals along the [0 0 1] direction was preferred, resulting in a necklace shape nanocrystal.

Recently, researchers have also synthesized one-dimensional metal oxide nanocrystals through a nonhydrolytic route. Cheon and Alivisatos et al. reported the shape evolution of titanium dioxide nanocrystals from bullet and diamond structures to rods structures by the modulation of surface energies of the different crystallographic faces through the use of a surface selective capping molecule [31]. As shown in Fig. 8, the shape of the obtained nanocrystals evolves from bullet to diamond, rod, and branched rod according to the concentration of capping molecule (Fig. 8). The observed structural growth patterns suggest that the injection of the titanium isopropoxide precursor into the reaction solution induces the formation of TiO_2 truncated octahedral bipyramid seeds terminated by {0 0 1} faces with high surface energy and {1 0 1} faces with relatively low surface energy. Then, the final shape of anatase nanocrystals is governed by the competition between the relative surface energies of the {0 0 1} and {1 0 1} faces, and therefore, the growth rate ratio between [0 0 1] and [1 0 1] directions (G_{001} and G_{101}, respectively). In the absence of lauric acid (LA) or at low lauric acid concentrations (<2 mmol), the ratio between the growth rates along the [0 0 1] and [1 0 1] directions is larger than the ratio between the *c* and *a* lattice parameters ($G_{100} \gg 2.7G_{101}$), thus bullet and diamond shapes arise from the shrinking of the {0 0 1} faces and the complete elimination of {0 0 1} faces at one or two ends of the truncated octahedral bipyramid seed, respectively. The diamond shape allows the crystal to expose only {1 0 1} faces, which are the lowest energy ones, as indicated by the fact that natural anatase crystals facet to expose ⟨1 0 1⟩ planes. At high LA concentration, however, LA selectively and strongly binds to the {0 0 1} faces through a bridge-bonding mode and slows down the growth along the ⟨0 0 1⟩ directions. When the growth rate along the [0 0 1] direction is close to 2.7 times that along the [1 0 1] direction ($G_{100} = \sim 2.7G_{101}$), two Ti layers grow along the [0 0 1] direction during the time of four Ti layers' growth along the [1 0 1] direction, according to crystal symmetry. Under this condition, monomers continuously grow further onto both {0 0 1} faces and {1 0 1} faces of the truncated octahedral bipyramid seeds, in such a way to expand the {1 0 1} faces during crystal growth while preserving a constant {0 0 1} surface area. However, when the (1 0 1) surface area reaches a critical value under the kinetically driven regime, the formation of a step instead of further homogeneous expansion of (1 0 1) surfaces leads to the growth of faceted rods. This study suggests that the surface

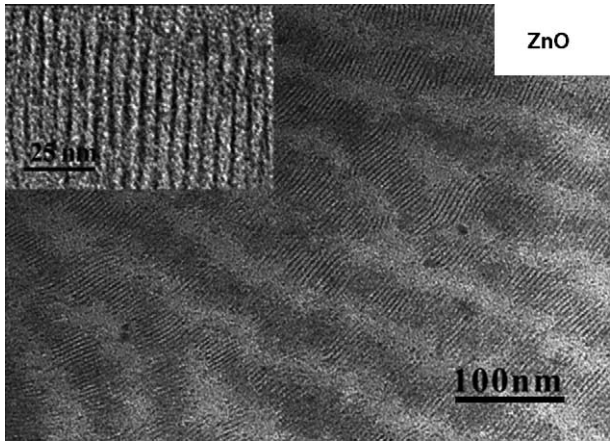

Fig. 9. Self-assembled ZnO nanorods. (Reprinted in part with permission from ref. [32]. Copyright 2004 American Chemical Society.)

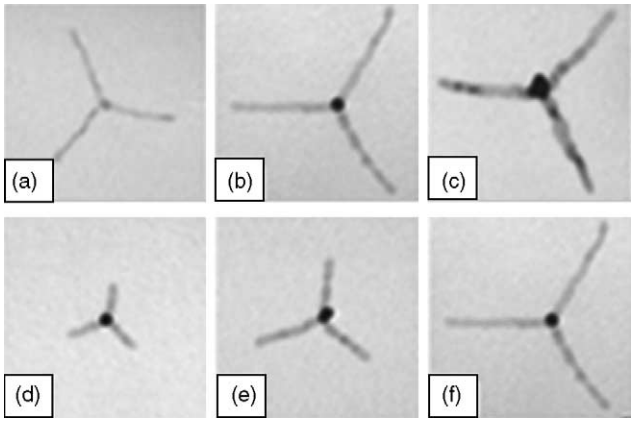

Fig. 10. Various CdTe tetrapod nanocrystals. (a–c) A series of tetrapods having comparable arm lengths but different diameters. (d–f) A series of tetrapods comparable arm diameters but different lengths. (Reprinted in part with permission from ref. [34]. Copyright 2003 Nature.)

energy control by capping molecules is a powerful tool for tailoring nanocrystal shape even in the case of metal oxides.

Other one-dimensional metal oxide nanocrystals also synthesized through the nonhydrolytic method. O'Brien and co-workers reported the synthesis of zinc oxide nanorods with a high degree of crystallinity and a narrow size distribution [32]. The nanocrystals could be assembled into separate close-packed "stacks", which they align with the long axis parallel to each other (Fig. 9).

A cubic–perovskite structured transition metal oxide is important due to its unique electronic, magnetic, and optical properties. The one-dimensional ternary perovskite oxide was first demonstrated in solution-based synthesis by Park and co-workers [33]. They synthesized single-crystalline cubic perovskite $BaTiO_3$ and $SrTiO_3$ by solution phase decomposition of bimetallic precursors in the presence of stabilizing ligands.

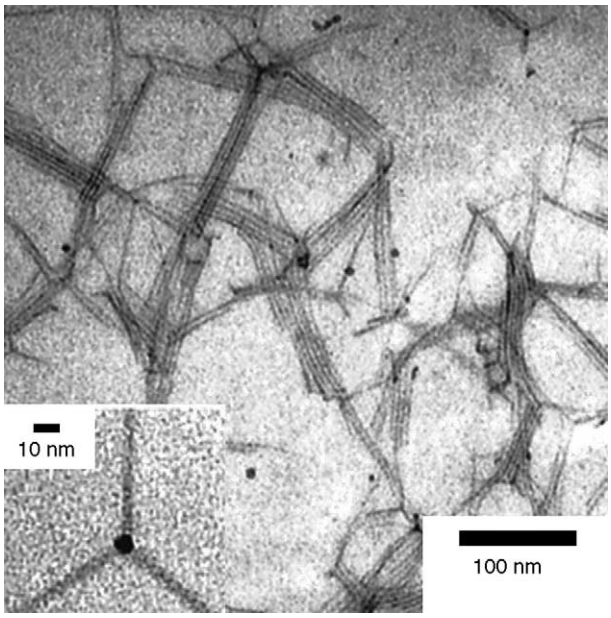

Fig. 11. MnS wire-based tetrapods. (Reprinted in part with permission from ref. [20]. Copyright 2002 American Chemical Society.)

2.2. Novel nano-building structures

As described above, shape controls of one-dimensional rods and wires nanocrystals have been widely studied. These basic building blocks have unique geometry and properties with their shapes and they can be used as components of nano-building structures. If the assemblies of each component with different geometries can be controlled, construction of novel nano-building structures may be possible. For example, L-shaped structures can be obtained using two rods and a cube and V-shaped structures can be achieved by assembling two rods and a tetrahedron. CdSe, CdTe tetrapods obtained by Alivisatos (Fig. 10) and CdS, MnS tetrapods by Cheon, respectively, are a good example of such a nanosystem [19,20]

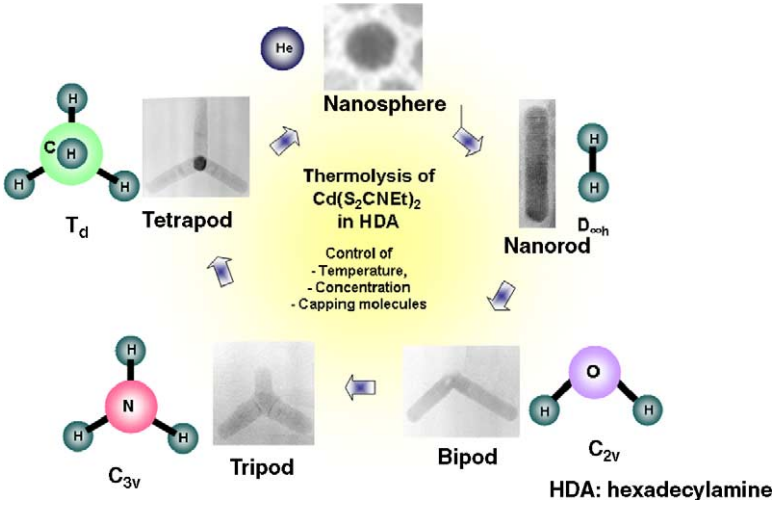

Fig. 12. CdS multipods with various symmetries. The nanocrystals shape changes form isotropic sphere to rod, bipod, tripod, and tetrapod. (Reprinted in part with permission from ref. [19]. Copyright 2001 American Chemical Society.)

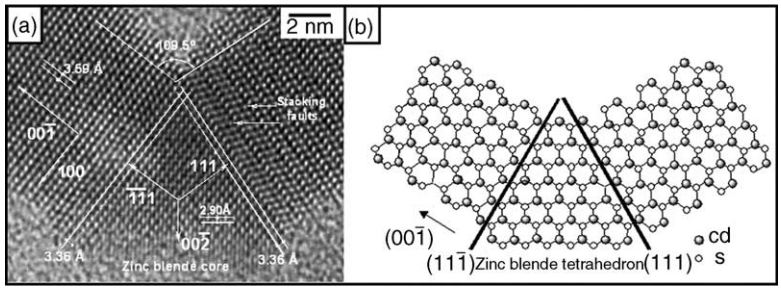

Fig. 13. Atomic structure of bipod shaped nanocrystals. (a) A HRTEM image of CdS tetrapods and (b) 2D projected model of bipod shaped CdS nanocrystals. (Reprinted in part with permission from ref. [19]. Copyright 2001 American Chemical Society.)

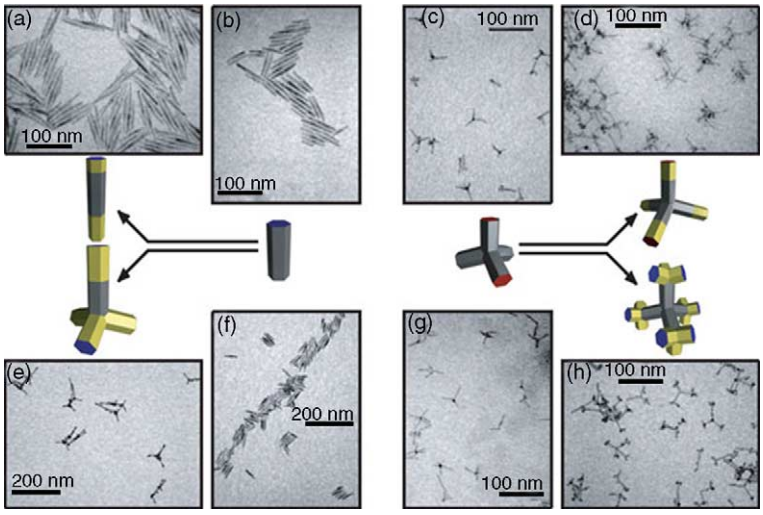

Fig. 14. Multi-component heterostructures of one-dimensional shapes. Survey of nanocrystal heterostructures. Extended rods (a) were formed first by growing CdS nanorods (b), then adding CdSe extensions to each end. Branched rods (e) result from nucleation of CdTe on either end of CdSe nanorods (f). A CdTe zincblende region at one end creates the branch point. CdSe tetrapods (c and g) comprise a zincblende core and four wurtzite arms. Extending each arm linearly with CdTe yields extended tetrapods (d). Branched tetrapods (h) result from nucleation of CdTe zincblende branch points on the end of each arm. The model sequences illustrate the growth processes. In each case, the first generation is shown in grey and the second in yellow, while red and blue indicate the unique crystal faces of the wurtzite structure. (Reprinted in part with permission from ref. [35]. Copyright 2004 Nature.)

(Fig. 11). Under certain conditions, zinc blende tetrahedron seeds with four {1 1 1} faces and subsequent rod growth on these four surfaces resulted in tetrapod shaped nanocrystals with tetrahedral (T_d) symmetry [15,19,34]. Wire formation of MnS instead of rod-shaped nanocrystals arises from a larger surface energy difference between the {0 0 1} faces of wurtzite due to the unoccupied d orbitals of the surface manganese metals [20].

Formation of novel multipod structures using a tetrahedron and one-dimensional rods were thoroughly studied in the case of CdS nanocrystals. Kinetic controlled growth resulted in a systematic variation of novel structures from spheres to 1D rod, bipod, tripod, and tetrapod with corresponding point symmetry of $D_{\infty h}$, C_{2v}, T_d, and C_{3v}, respectively (Figs. 12 and 13).

Heterostructures with one-dimensional shapes are of great interest because these nanocrystals permit more complexity and multiple functionalities. Very recently, multi-component one-dimensional structures with linear and branched topology synthesized by Alivisatos and co-workers [35]. Epitaxial growth of wurtzite CdSe from the CdS nanorod seeds with yields CdSe/CdS/CdSe nanorods, while the nucleation of zinc blende CdTe from the CdSe nanorod ends, which follows wurtzite CdTe arm growth, results in extended CdTe/CdSe/CdTe tetrapods (Fig. 14). When CdSe tetrapods are used as a seed for the CdTe nanocrystal growth, more

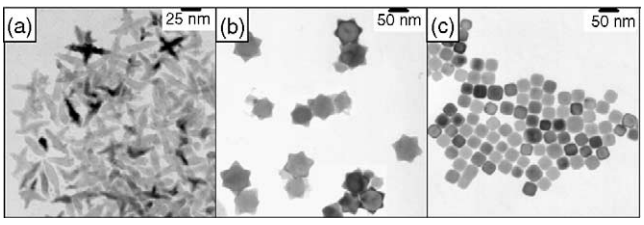

Fig. 15. TEM images of (a) rod-based multipods, (b) star-shaped nanocrystals, and (c) cubes. (Reprinted in part with permission from ref. [10]. Copyright 2002 American Chemical Society.)

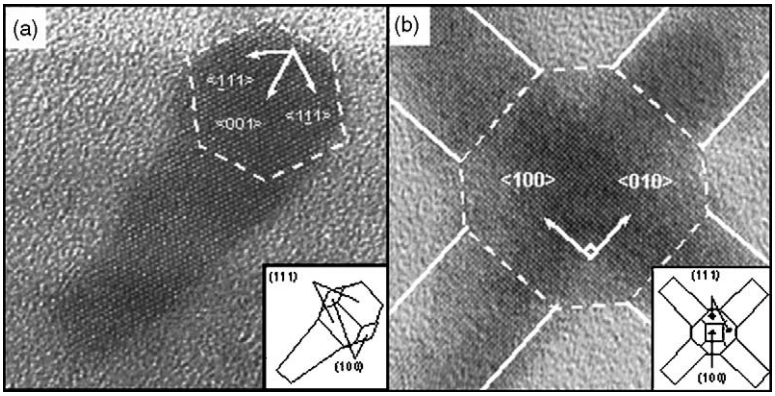

Fig. 16. (a) A HRTEM image of tadpole shaped monopod with zone axis of [1 1 0]. (b) A HRTEM image of cross-shaped tetrapod of PbS nanocrystals with zone axis of [0 0 1]. (Reprinted in part with permission from ref. [10]. Copyright 2002 American Chemical Society.)

complex shapes of nanocrystals are obtained. Extending each arm linearly with wurtzite CdTe nanocrystals results in extended tetrapods, while the nucleation of CdTe zinc blende branch points on the end of each CdSe arm yields branched tetrapods.

Geometrical control of these novel nano-building blocks is accomplished by carefully controlling nanocrystal growth parameters such as growth temperature, monomer concentration, and functional group of stabilizers. Geometrical shape evolution of isotropic rock salt structured PbS nanocrystals is a good example [10]. Rapid injection of a PbS molecular precursor induces the formation of tetradecahedron seeds that are terminated by {1 0 0} and {1 1 1} faces and subsequent competitive growth on these two different types of crystalline faces determines the final shape. Typically, in the rock salt structure, the {1 1 1} surface has a higher surface energy than the {1 0 0} surface. When excess thermal energy is supplied by utilizing high growth temperatures (e.g., $E = kT$, $T \sim 250\,^{\circ}C$), the thermodynamic regime governs the growth process and, due to faster growth on the {1 1 1} faces, the formation of cube shaped PbS nanocrystals is favored (Fig. 15(c)). However, in the presence of a strongly binding capping molecule (e.g., dodecanethiol), the thiol molecule binds to the {1 1 1} surface via a μ^3-Pb_3-SR bridging mode while weakly binding to the {1 0 0} faces. The surface energy of the {1 1 1} faces can selectively be lowered significantly relative to that of the {1 0 0} faces. Therefore, under the conditions of low temperature ($\sim 120\,^{\circ}C$) and in the presence of a strongly binding dodecanethiol capping molecule, the growth process shifts into the kinetic growth regime, and growth on the {1 0 0} faces with high surface energy is preferred. This results in 1D rod based single- and multi-pod structures (Fig. 15(a)). HRTEM images of multi-pods can be good evidence for the preferable growth along the [1 0 0] directions. The image of tadpole shaped nanocrystals and lattice distance measurements indicates that the rod grows along the ⟨0 0 1⟩ direction. Hexagonal shape of the truncated octahedral seed with four {1 1 1} and two {1 0 0} faces was observed (Fig. 16(a)). In the case of the cross-shaped nanocrystals, [1 0 0] directional growth was also observed. The separation angle between the pods of the cross is 90° and an octagonal shape consistent with the [0 0 1] projection of a tetradecahedron is observed at the central junction of the cross (Fig. 16(b)). Moreover, at intermediate temperatures (e.g., 180 °C), as a transient species, star-shaped nanocrystals possessing both the characteristics of 0D and 1D structures are formed (Fig. 15(b)).

3. Conclusions

In the past decade, various synthetic methodologies have been successfully developed for building novel nanostructures ranging from spheres and 1D rods to highly sophisticated novel architectures. Although recent studies have demonstrated that the ability to control complex nanostructures such as hollow cubes, stars, multi-pods is possible, a more comprehensive understanding of their growth mechanisms and the development of advanced synthetic schemes for the desired nano-building blocks are of critical importance for the continuous success and advancement of this field. Once there are enough nano-building blocks, or nano-'Legos', and different building components available to us, the rational assembly and manipulation of them into specific systems would follow. Futuristic nanodevices with novel applications would then be closer to realization.

Acknowledgements

We would like to thank Dr. Y.J. Kim, J.G. Kim, and K.T. Song (KBSI) for TEM. This work is supported in part by the Basic Research Program of KOSEF (Grant R02-2004-000-10096-0 (2004)), National R & D Project for Nano Science and Technology, AORAD (FA520904P0406), National R & D Program for Cancer Control of Ministry of Health & Welfare (Grant 0320250-2), Korea Health 21 R & D Project of Ministry of Health & Welfare (Grant 0405-MN01-0604-0007), and National Core Research Center for Nanomedical Technology (Grant R15-2004-024-02002-0).

References

[1] MRS Bull. 23 (1998) 15.
[2] G. Markovich, C.P. Collier, S.E. Henrichs, F. Remacle, R.D. Levine, J.R. Heath, Acc. Chem. Res. 32 (1999) 415.
[3] R. Jin, Y. Cao, C.A. Mirkin, K.L. Kelly, G.C. Schatz, J.G. Zheng, Science 294 (2001) 1901.
[4] A.N. Goldstein, C.M. Echer, A.P. Alivisatos, Science 256 (1996) 1425.
[5] H.W.Ch. Postma, T. Teepen, Z. Yao, M. Grifoni, C. Dekker, Science 293 (2001) 76.
[6] Y. Huang, X.F. Duan, Y. Cui, L.J. Lauhon, K.H. Kim, C.M. Lieber, Science 294 (2001) 313.
[7] T. Eckes, K. Kim, E. Joselevich, G.Y. Tseng, C.L. Cheung, C.M. Lieber, Science 289 (2000) 94.
[8] J.S. Bradley, B. Tesche, W. Busser, M. Maase, M.T. Reetz, J. Am. Chem. Soc. 122 (2000) 4631.
[9] V.F. Puntes, D. Zanchet, C.K. Erdonmez, A.P. Alivisatos, J. Am. Chem. Soc. 124 (2002) 12874.
[10] S.-M. Lee, Y. Jun, S.-N. Cho, J. Cheon, J. Am. Chem. Soc. 124 (2002) 11244.
[11] A.T. Hubbard, , in: T. Sugimoto (Ed.), Surfactant Science Series, vol. 92, Marcel Dekker Inc., New York, Basel, 2000.
[12] N. Chestnoy, R. Hull, L.E. Brus, J. Chem. Phys. 85 (1986) 2237.
[13] C.B. Murray, D.J. Norris, M.G. Bawendi, J. Am. Chem. Soc. 115 (1993) 8706.
[14] X. Peng, L. Manna, W. Yang, J. Wickham, E. Scher, A. Kadavanich, A.P. Alivisatos, Nature 404 (2000) 59.
[15] L. Manna, E. Scher, A.P. Alivisatos, J. Am. Chem. Soc. 122 (2000) 12700.
[16] Z. Tang, N.A. Kotov, M. Giersig, Science 297 (2000) 237.
[17] J.D. Holmes, K.P. Johnston, R.C. Doty, B.A. Korgel, Science 287 (2000) 1471.
[18] Y. Jun, C.-S. Choi, J. Cheon, Chem. Commun. 1 (2001) 101.
[19] Y. Jun, S.-M. Lee, N.-J. Kang, J. Cheon, J. Am. Chem. Soc. 123 (2001) 5150.
[20] Y. Jun, Y. Jung, J. Cheon, J. Am. Chem. Soc. 124 (2002) 615.
[21] C. Pacholski, A. Kornowski, H. Weller, Angew. Chem. Int. Ed. 41 (2002) 1188.
[22] C.-Y. Yeh, Z.W. Lu, S. Froyen, A. Zunger, Phys. Rev. B 46 (1992) 10086.
[23] Y.-H. Kim, Y. Jun, B.-H. Jun, S.-M. Lee, J. Cheon, J. Am. Chem. Soc. 124 (2002) 13656.
[24] T.J. Trentler, S.C. Goel, K.M. Hickman, A.M. Viano, M.Y. Chiang, A.M. Beatty, P.C. Gibbons, W.E. Buhro, J. Am. Chem. Soc. 119 (1997) 2172.
[25] S. Kan, T. Mokari, E. Rothenberg, U. Banin, Nat. Mater. 2 (2003) 155.
[26] A.M. Morales, C.M. Lieber, Science 279 (1998) 208.
[27] T. Hanrath, B.A. Korgel, J. Am. Chem. Soc. 124 (2002) 1424.
[28] D. Gerion, N. Zaitseva, C. Saw, M.F. Casula, S. Fakra, T.V. Buuren, G. Galli, Nano Lett. 4 (2004) 597.
[29] A. Chemseddine, T. Moritz, Eur. J. Inorg. Chem. (1999) 235.
[30] R.L. Penn, J.F. Banfield, Geochim. Et Cosmochim. Acta 63 (1999) 1549.
[31] Y. Jun, M.F. Casula, J.-H. Sim, S.Y. Kim, J. Cheon, A.P. Alivisatos, J. Am. Chem. Soc. 125 (2003) 15981.
[32] M. Yin, Y. Gu, I.L. Kuskovsky, T. Andelman, Y. Zhu, G.F. Neumark, S. O'Brein, J. Am. Chem. Soc. 126 (2004) 6206.
[33] J.J. Urban, W.S. Yun, Q. Gu, H. Park, J. Am. Chem. Soc. 124 (2002) 1186.
[34] L. Manna, D.J. Milliron, A. Meisel, E.C. Scher, A.P. Alivisatos, Nat. Mater. 2 (2003) 382.
[35] D.J. Milliron, S.M. Hughes, Y. Cui, L. Manna, J. Li, L.-W. Wang, A.P. Alivisatos, Nature 430 (2004) 190.